Published in final edited form as:

Cell Rep. 2015 February 10; 10(5): 783–795. doi:10.1016/j.celrep.2015.01.015.

Activity-Dependent Ubiquitination of GluA1 and GluA2 Regulates AMPA Receptor Intracellular Sorting and Degradation

Jocelyn Widagdo[1], **Ye Jin Chai**[1,2], **Margreet C. Ridder**[1], **Yu Qian Chau**[1,2], **Richard C. Johnson**[3], **Pankaj Sah**[1], **Richard L. Huganir**[3,4,*], and **Victor Anggono**[1,2,4,*]

[1]Queensland Brain Institute, The University of Queensland, Brisbane, QLD 4072, Australia

[2]Clem Jones Centre for Ageing Dementia Research, The University of Queensland, Brisbane, QLD 4072, Australia

[3]Department of Neuroscience, Johns Hopkins University School of Medicine, Baltimore, MD 21205, USA

SUMMARY

AMPA receptors (AMPARs) have recently been shown to undergo post-translational ubiquitination in mammalian neurons. However, the underlying molecular mechanisms are poorly understood and remain controversial. Here, we report that all four AMPAR subunits (GluA1–4) are rapidly ubiquitinated upon brief application of AMPA or bicuculline in cultured neurons. This process is Ca^{2+} dependent and requires the activity of L-type voltage-gated Ca^{2+} channels and Ca^{2+}/calmodulin-dependent kinase II. The ubiquitination of all subunits occurs exclusively on AMPARs located on the plasma membrane post-endocytosis. The sites of ubiquitination were mapped to Lys-868 in GluA1 and Lys-870/Lys-882 in GluA2 C-terminals. Mutation of these lysines did not affect basal surface expression or AMPA-induced internalization of GluA1 and GluA2 subunits. Instead, it reduced the intracellular trafficking of AMPARs to the late endosomes and thus protein degradation. These data indicate that ubiquitination is an important regulatory signal for controlling AMPAR function, which may be crucial for synaptic plasticity.

INTRODUCTION

AMPA receptors (AMPARs) are tetrameric assemblies of homologous subunits encoded by four different genes, GluA1–4, which combine in different stoichiometries to form functional receptor subtypes. AsAMPARs mediate the vast majority of fast excitatory

*Correspondence: rhuganir@jhmi.edu (R.L.H.), v.anggono@uq.edu.au (V.A.).
[4]Co-senior author

SUPPLEMENTAL INFORMATION

Supplemental Information includes five figures and can be found with this article online at http://dx.doi.org/10.1016/j.celrep.2015.01.015.

AUTHOR CONTRIBUTIONS

J.W., R.L.H., and V.A. designed the research; J.W. and V.A. performed all the biochemistry experiments; J.W., Y.J.C., and V.A. executed and analyzed all the immunostaining experiments; and M.C.R. performed the electrophysiological recordings and analysis supervised by P.S. and V.A. J.W., Y.Q.C., and R.C.J. contributed new reagents. V.A. wrote the manuscript with input from all authors.

synaptic transmission in the mammalian CNS, the regulation of AMPAR density at the post-synaptic membrane is recognized as one of the key mechanisms underlying activity-dependent changes in synaptic strength (Huganir and Nicoll, 2013). The number of synaptic AMPARs is dependent on the relative rates of receptor biosynthesis, exocytosis, lateral diffusion, endocytosis, and degradation (Shepherd and Huganir, 2007). Surface AMPARs are internalized via clathrin-mediated endocytosis, followed by intracellular trafficking and sorting through recycling or late endosomes. Consequently, AMPARs are recycled back to the plasma membrane or degraded in the lysosome, respectively (Ehlers, 2000; Lee et al., 2004). This dynamic trafficking of AMPARs into and out of synapses is tightly regulated by subunit-specific AMPAR-interacting proteins as well as various post-translational modifications that occur on their cytoplasmic C-terminal domains (Anggono and Huganir, 2012; Lu and Roche, 2012). However, the exact molecular mechanisms that determine activity-dependent AMPAR intracellular sorting into recycling and late endosomes remain poorly understood.

Ubiquitination, a reversible post-translational modification that involves the covalent attachment of a 76-amino-acid ubiquitin to lysine residues of a substrate protein, is known to regulate a myriad of physiological processes, including protein degradation, endocytosis, and the sorting and trafficking of transmembrane proteins (Hershko and Ciechanover, 1998). Previous studies have demonstrated an important role for the ubiquitin-proteasome system (UPS) in regulating AMPAR trafficking and turnover (Fu et al., 2011; Hou et al., 2011; Patrick et al., 2003; Yuen et al., 2012; Zhang et al., 2009). The *C. elegans* non-NMDA-type glutamate receptor GLR-1, which is most similar to mammalian AMPARs, was first shown to be ubiquitinated to regulate the number of glutamate receptors at synapses (Burbea et al., 2002). More recently, several studies have demonstrated direct ubiquitination of AMPARs in mammalian central neurons (Lin et al., 2011; Lussier et al., 2011; Schwarz et al., 2010). However, these studies have yielded conflicting and inconsistent data. Schwarz et al. (2010) reported that the GluA1, but not the GluA2, subunit was ubiquitinated by the E3-ligase Nedd4–1 to promote ligand-induced internalization and sorting of AMPARs. In contrast, Lussier et al. (2011, 2012) found that it was the GluA2, but not the GluA1, subunit of AMPARs that underwent activity-dependent ubiquitination post-endocytosis. As a result, several fundamental questions have remained unanswered with regards to which AMPAR subunits are ubiquitinated, and when this occurs, as well as the site of ubiquitination and the functional effects of this process.

RESULTS

All Four AMPAR Subunits Are Ubiquitinated in an Activity- and Ca^{2+}-Dependent Manner

To determine which AMPAR subunits are ubiquitinated in mammalian neurons, we first performed the conventional ubiquitination assay, which involved immunoprecipitating GluA1 and GluA2 subunits from neuronal lysates that had been treated with 100 μM AMPA in the presence of 100 μM D,L-APV plus 1 μM tetrodotoxin (TTX) (for 2 min before switching to artificial cerebrospinal fluid/ACSF solution containing APV and TTX for 8 min, hereafter referred to as AMPA treatment). We found that both the GluA1 and GluA2 subunits were robustly ubiquitinated following AMPA treatment (Figure S1A). This assay

was carried out under denaturing conditions in which neurons were lysed in 1% SDS to ensure complete dissociation of the GluA1/2 AMPAR complex (Figure S1B). To confirm these findings, we performed a reversed immunoprecipitation assay with anti-ubiquitin antibodies on AMPA-treated neuronal lysates and blotted them with specific antibodies against the GluA1 subunit. We observed high-molecular-weight GluA1 immunoreactivity in the AMPA-treated lysates, which was absent in the control lane, indicative of a ubiquitinated GluA1 signal (Figure 1A). Using this assay, we next treated cortical neurons with a variety of agents that activate glutamate receptors, immunoprecipitated the lysates with anti-ubiquitin antibodies, and blotted with specific antibodies against the GluA1–4 subunits (Figure S1C). We found that all four AMPAR subunits were rapidly ubiquitinated in neurons that were incubated in the presence of AMPA or the $GABA_A$ receptor antagonist, bicuculline (40 μM), albeit at a lower level compared to AMPA treatment; this did not occur in the presence of an NMDA receptor (NMDAR) agonist (20 μM NMDA plus 1 μM TTX) or the metabotropic glutamate receptor (mGluR) agonist DHPG (100 μM; Figure 1B). Taken together, these results unequivocally demonstrate that activation of AMPARs induces ubiquitination on all AMPAR subunits, essentially resolving the issue of which AMPAR subunit gets ubiquitinated.

To determine whether ubiquitination occurs on surface AMPARs, we treated neurons with NHS-SS-biotin to label all surface proteins prior to 10 min incubation with AMPA or bicuculline. Neuronal lysates were then subjected to two rounds of affinity purification with neutravidin agarose beads to deplete all surface proteins, followed by immunoprecipitation with anti-ubiquitin antibodies. We found that AMPAR ubiquitination was absent in the neuronal lysates that were pre-treated with biotin but were present in the control samples, suggesting that the ubiquitination of GluA1–4 subunits occurs exclusively on AMPARs that are located on the plasma membrane (Figure 1C). Consistent with previous studies (Lussier et al., 2011; Schwarz et al., 2010), we also found that ubiquitination of AMPARs is Ca^{2+} dependent as the treatment of cortical neurons with AMPA or bicuculline failed to induce AMPAR ubiquitination in ACSF solution containing no extracellular Ca^{2+} and the Ca^{2+} chelators, EGTA and BAPTA-AM (Figure 1D).

Our data show that both AMPA and bicuculline treatment reproducibly induce AMPAR ubiquitination in a Ca^{2+}-dependent manner. Both treatments result in the activation of AMPARs either by direct binding of the ligand or by release of glutamate following blockade of inhibitory synaptic transmission. To investigate the signaling pathways underlying AMPAR ubiquitination, we treated neurons with ionotropic glutamate receptor and L-type voltage-gated calcium channel (L-VGCC) blockers. We found that the agonist-induced AMPAR ubiquitination was blocked by the AMPAR antagonist, NBQX, and the L-VGCC blocker, nimodipine, but not by the NMDAR antagonist, APV (Figures 1E and 1G). Interestingly, bicuculline-induced ubiquitination of AMPARs requires the activation of AMPARs, NMDARs, L-VGCCs, and, to a lesser extent, group I mGluRs, as shown by the inhibitory effects of NBQX, APV, nimodipine, Bay 36–7620, and MPEP (Figures 1F and 1H). These results show that the release of glutamate activates AMPARs and NMDARs, with consequent depolarization and activation of L-VGCCs, and that the resultant Ca^{2+} influx initiates ubiquitination of AMPARs, which can also be modulated by mGluR signaling.

Ca^{2+} influx into the post-synaptic compartment is known to activate Ca^{2+}-dependent kinases, such as CaMKII, which interacts with NMDARs and L-VGCCs to mediate synaptic plasticity (Hell, 2014). To test whether CaMKII is the downstream effector of Ca^{2+}, we treated neurons with KN-93 to inhibit CaMKII activity before adding AMPA or bicuculline. We found that inhibiting CaMKII activity strongly attenuated AMPAR ubiquitination (Figures 1I–1L). Together, these data suggest that CaMKII is critical for activity-dependent ubiquitination of AMPARs.

GluA1 and GluA2 Are Ubiquitinated on C-Terminal Lysine Residues

To determine the specific role of ubiquitination on AMPAR function, we first mapped the specific lysine residues to which ubiquitin is covalently attached on the GluA1 and GluA2 subunits. All lysine residues in the GluA1 and GluA2 C-terminal tails were initially mutated to arginines either individually or in combination (Figure 2A). To achieve high transfection efficiency, we electroporated cortical neurons with cDNA constructs encoding pH-sensitive GFP-tagged GluA1 (pH-GluA1) or pH-GluA2 (either wild-type [WT] or mutant) at days in vitro (DIV) 0. At DIV13, neurons were treated with AMPA, lysed, and immunoprecipitated with anti-GFP antibodies. This assay was done under denaturing conditions to avoid co-immunoprecipitation of endogenous AMPARs (Figures 2B and 2D). We found that AMPA-induced ubiquitination of GluA1 and GluA2 subunits was completely abolished in mutants in which all lysine residues were mutated to arginines (GluA1-K813/819/822/868R, 0.7% ± 0.9% of WT; GluA2-K838/844/847/850/870/882R, 8.2% ± 6.3% of WT; Figures 2B–2E). This suggests that the ubiquitination of AMPAR subunits occurs in the C-terminal domain, ruling out the involvement of the extracellular N-terminal or transmembrane domain. Systematic analysis of each individual lysine mutation in GluA1 and GluA2 revealed that Lys-868 of GluA1 (19.5% ± 9.4% of WT) and Lys-870 (48.5% ± 13.0% of WT) and Lys-882 (48.0% ± 19.8% of WT) of GluA2 are the major sites of ubiquitination (Figures 2B–2E). Furthermore, GluA2 K870/882R double mutants had an additive effect in reducing AMPA-induced GluA2 ubiquitination (19.3% ± 8.8% of WT; Figures 2D and 2E). Interestingly, these lysine residues are located in the distal C-terminal domains of GluA1 and GluA2 and are not conserved between the two subunits. These data provide us with molecular tools for investigating the role of ubiquitination in regulating AMPAR function.

Ubiquitination of GluA1 and GluA2 Does Not Regulate AMPAR Surface Expression and Agonist-Induced Endocytosis

We next determined the steady-state surface expression of GluA1 and GluA2 ubiquitin-deficient mutants (GluA1 K868R, GluA2 K870R, GluA2 K882R, and GluA2 K870/882R) to investigate whether the loss of AMPAR ubiquitination altered the trafficking of AMPARs under basal conditions. To do this, we overexpressed pH-GluA1 or pH-GluA2, either WT or mutants, in mature hippocampal neurons and performed surface staining with anti-GFP antibodies that recognize the extracellular pHluorin. We did not observe any significant change in the surface/total ratio of GluA1/2 ubiquitin-deficient mutants compared with WT (Figures 3A, 3B, 3F, and 3G). Consistent with the above findings, there was no significant difference in the miniature excitatory post-synaptic current (mEPSC) amplitude and frequency in neurons expressing pH-GluA1 or pH-GluA2 mutants compared with WT neurons (Figures 3C–3E and 3H–3J). Together, these results indicate that direct

ubiquitination of GluA1 and GluA2 on C-terminal Lys-868 and Lys-870/Lys-882 is not required for the basal trafficking and synaptic targeting of AMPARs in hippocampal neurons.

As ubiquitination of transmembrane receptors often leads to their internalization, we then examined whether ubiquitination of GluA1 and GluA2 regulated the agonist-induced AMPAR endocytosis. To test this possibility, we transfected neurons with pH-GluA1 or pH-GluA2, either WT or ubiquitin-deficient mutants, and performed the fluorescence-based antibody-feeding assay with GFP antibodies to measure the degree of intracellular accumulation of endocytosed receptors following AMPA treatment. We found that mutations of GluA1 and GluA2 C-terminal lysine residues had no effect on the ligand-induced AMPAR endocytosis (Figures 4A–4D). To investigate whether activity-dependent ubiquitination of AMPARs occurs pre- or post-endocytosis, we treated neurons with dynasore, a dynamin blocker that inhibits its GTPase activity (Macia et al., 2006), and found that both AMPA- and bicuculline-induced ubiquitination of all AMPAR subunits were abolished (Figure 4E). Collectively, these data demonstrate that activity-dependent ubiquitination of AMPARs occurs after internalization, which explains the lack of effect of the GluA1 and GluA2 ubiquitin-deficient mutants on AMPA-induced internalization.

Ubiquitination of GluA1 and GluA2 Is Required for the Intracellular Sorting of AMPARs to Late Endosomes for Degradation

Previous studies have shown that AMPAR activation targets receptors to late endosomes, with subsequent degradation in lysosomes (Ehlers, 2000; Schwarz et al., 2010). Based on the above findings, we determined whether ubiquitination was involved in sorting internalized AMPARs into late endosomes. To do this, we transfected mature hippocampal neurons with pH-GluA1, either WT or K868R, and performed immunofluorescence detection of internalized pH-GluA1 that co-labelled for early (EEA1; 5 min), recycling (syntaxin-13; 10 min), or late endosomes (LAMP-1; 30 min). Soon after AMPA-induced internalization, the majority of pH-GluA1 WT and K868R showed strong co-localization patterns with early and recycling endosome markers (Figures 5A–5C). However, by 30 min, the transport of pH-GluA1 K868R to LAMP-1-positive late endosomes was significantly reduced compared to WT (WT, 36.2% ± 2.8%; K868R, 23.9% ± 3.5%; Figures 5A and 5D). Instead, we found that the non-ubiquitinated pH-GluA1 K868R recycled back to the plasma membrane, resulting in a higher expression level of AMPARs following agonist-induced internalization compared to WT (WT, 63.2% ± 8.3%; K868R, 97.4% ± 8.0%; Figures S2A and S2B). These observations indicate that ubiquitination of the GluA1 subunit dictates the intracellular transport of internalized AMPARs to late endosomes, which are subsequently degraded in lysosomes.

The reduction in agonist-induced late endosomal targeting of AMPARs was also observed for the GluA2 ubiquitin-deficient mutants (WT, 25.2% ± 4.2%; K870R, 8.3% ± 2.5%; K882R, 7.6% ± 2.1%; K870/882R, 10.8% ± 3.6%; Figures 5E and 5F), which showed normal intracellular sorting into early and recycling endosomes (Figures S3A–S3D). Unlike for GluA1, however, we did not detect any significant difference in the surface expression of pH-GluA2 WT and K870/882R mutant post-endocytosis (Figure S2C). In our assay, we

found that pH-GluA2 rapidly recycled back to the surface after endocytosis. Consistent with a previous report (Lee et al., 2004), these data suggest that intracellular accumulation of GluA2 quickly reaches a steady state at a low level. The effect on endosomal sorting may result from a gradual accumulation of rapidly recycling GluA2 over a longer period of time. It is also plausible that GluA2 ubiquitination may occur at a relatively low level compared to that of GluA1, which could preclude the detection of GluA2-containing receptors that do not recycle back to the plasma membrane.

Ubiquitin has seven lysine residues (K6, K11, K27, K29, K33, K48, and K63), all of which can form polyubiquitin chains, resulting in different types of ubiquitin linkages and structures that alter the function of the target protein in different ways (Haglund and Dikic, 2005). For example, the attachment of K48-linked polyubiquitin chains typically targets protein substrates to the proteasome, whereas formation of K63 chains directs proteins through endosomal trafficking into lysosomes (Nathan et al., 2013). To determine the types of ubiquitin linkages preferentially attached to AMPARs, we examined GluA1 and GluA2 ubiquitination using specific antibodies that recognize the two major types of ubiquitin chain, K48- and K63-linked chains. As shown in Figure S4, no signal corresponding to K48 chains was detected in GluA1 and GluA2 immunoprecipitates, whereas an increase in K63-linked ubiquitination was associated with these AMPAR subunits that were recovered from AMPA-treated neurons. These data corroborate our previous results that the ubiquitination of GluA1 and GluA2 targets AMPARs into late endosomes through the intracellular endosomal trafficking.

To test whether AMPAR ubiquitination ultimately leads to lysosomal targeting, we examined the degradation of GluA1 and GluA2 subunits in the presence of ligand. Cortical neurons were electroporated with pH-GluA1 or pH-GluA2, either WT or mutants, at DIV0 and were biotinylated to label surface proteins at DIV13. As expected, the addition of 100 μM AMPA caused the degradation of surface pH-GluA1 and pH-GluA2 (GluA1 WT, 76.5% ± 1.9%; GluA2 WT, 67.1% ± 8.9% of surface receptors remaining after 90 min; Figures 6A–6D). However, AMPA had no significant effect on the degradation of pH-GluA1 and pH-GluA2 ubiquitin-deficient mutants (GluA1 K868R, 113.4% ± 6.3%; GluA2 K870R, 89.3% ± 6.9%; GluA2 K882R, 112.3% ± 13.7%; GluA2 K870/882R, 109.1% ± 8.9% of remaining surface receptors; Figures 6A–6D). Interestingly, ubiquitination had no effect on basal protein turnover of AMPARs as determined by the levels of receptors remaining after 24 hr treatment with cycloheximide (50 μg/ml) in cortical neurons that had been electroporated with either WT or ubiquitin-defective pH-GluA1 or pH-GluA2 constructs (Figures S5A–S5D). Together with our immunostaining and western blot results, these experiments provide strong evidence for a role of ubiquitination in ligand-induced late endosomal targeting and lysosomal degradation of AMPARs.

DISCUSSION

Ubiquitination is a highly regulated and reversible post-translational modification that controls vital cellular processes in the brain, including activity-dependent remodelling of the post-synaptic density, synaptic plasticity, learning, and memory (Ehlers, 2003; Mabb and Ehlers, 2010). The AMPAR has recently been shown to be a direct target of ubiquitination in

mammalian central neurons (Lin et al., 2011; Lussier et al., 2011; Schwarz et al., 2010). However, the identity of the AMPAR subunit that undergoes ubiquitination remains controversial. Schwarz et al. (2010) found that the application of AMPA specifically promotes the ubiquitination of the GluA1, but not the GluA2 subunit. In contrast, Lussier et al. (2011) argue that the opposite is true, although they used bicuculline as a stimulus. These results contribute, at least partially, to the idea of subunit-specific regulation of AMPAR function by protein ubiquitination. Our data provide an explanation for these different findings and indicate that ubiquitination of AMPARs is not subunit specific. We show that all of the AMPAR subunits, GluA1–4, are directly ubiquitinated following either AMPA or bicuculline stimulation. The discrepancies among previous studies can be explained by their use of GluA1 and GluA2 antibodies raised against different epitopes, namely the N- or the C-terminal domains. Here, we used N-terminal GluA1 and GluA2 antibodies, whereas Lussier et al. (2011) utilized C-terminal antibodies for the immunoprecipitation assay. In our hands, the C-terminal GluA1 antibodies did not bind ubiquitinated receptor subunits (data not shown). Given the differential requirement for NMDAR activity during AMPA- and bicuculline-induced ubiquitination of AMPARs, we propose that the involvement of these two molecularly distinct signaling pathways may result in the recruitment of different E3 ligases (e.g., Nedd4-1, RNF167, or APC^{Cdh1}) and dictate the routes of AMPAR trafficking and subsequent degradation through the lysosomal or proteasomal pathways. Whether or not these E3 ligases can mediate the ubiquitination of GluA1 and GluA2 subunits and how they are activated by distinct neuronal stimuli and regulated by CamKII activity are currently unclear and need to be examined systematically.

Recent studies have suggested that ubiquitination of GluA1 and GluA2 subunits regulates surface and synaptic expression of AMPARs under basal conditions (Lin et al., 2011; Lussier et al., 2012; Schwarz et al., 2010). However, these studies rely on overexpression, knockdown, or mutational studies of Nedd4–1 and RNF167, which do not necessarily reflect the specific importance of AMPAR ubiquitination versus ubiquitination in general. In order to directly demonstrate a role for ubiquitination of GluA1 and GluA2 in regulating AMPAR function, we mapped the sites of ubiquitination by replacing each lysine residue with arginine in the C-terminal domains, either individually or in combination. We found that mutation of all C-terminal lysines completely abolished the agonist-induced ubiquitination of GluA1 and GluA2 in mammalian central neurons. Furthermore, we identified Lys-868 and Lys-870/Lys-882 as the major ubiquitination sites, mutations of which resulted in approximately 80% reduction in GluA1 and GluA2 ubiquitination, respectively. These ubiquitin-deficient mutants have no effect on the steady-state surface expression of AMPARs and AMPAR-mediated excitatory synaptic transmission in mature hippocampal neurons. Despite this, Schwarz et al. (2010) observed a significant increase in surface GluA1-4KR (all four lysines in the C-tail mutated to arginines) compared to GluA1-WT. In our hands, the same mutant did not affect the surface and synaptic GluA1 expression in neurons (data not shown), although the reasons for this difference remain clear.

It is widely believed that ubiquitination of many transmembrane receptors is crucial to promote their endocytosis (Sorkin and von Zastrow, 2009). Indeed, previous studies have reported that the ubiquitination of GluA1 is required for activity-induced internalization of surface AMPARs (Lin et al., 2011; Schwarz et al., 2010). Surprisingly, our experimental

data contradict those findings. First, we found that accumulation of internalized AMPARs is similar in neurons expressing WT or ubiquitin-defective GluA1/GluA2 mutants 10 min after AMPA treatment. In addition, GluA1-4KR and GluA2-6KR also display normal ligand-induced internalization, excluding the possibility that the residual ubiquitination (20% of maximum levels of receptor ubiquitination) could be sufficient to drive AMPAR endocytosis (data not shown). Second, activity-induced ubiquitination of all AMPAR subunits is completely abolished by a dynamin inhibitor, dynasore, a result that we have replicated using an independent dynamin GTPase blocker, Dynole (data not shown). Given that activity-induced internalization of AMPARs is dependent on dynamin GTPase activity (Carroll et al., 1999) and that ubiquitination exclusively involves a population of surface AMPARs, these data indicate that the activity-dependent ubiquitination of AMPARs must occur post-endocytosis. This result is in agreement with a recent report (Lussier et al., 2011) and explains why GluA1 and GluA2 ubiquitin-deficient mutants undergo normal internalization in neurons. Based on these findings, we conclude that ubiquitination is not required for agonist-induced endocytosis of AMPARs. Interestingly, direct ubiquitination of several transmembrane receptors from the receptor tyrosine kinase and the cytokine receptor superfamily, including the epidermal growth factor receptor, the fibroblast growth factor receptor, and the growth hormone receptor, is not required for their internalization (Govers et al., 1999; Haugsten et al., 2008; Huang et al., 2007). Instead, ubiquitination regulates their intracellular sorting into late endosomes and subsequent degradation in lysosomes. Indeed, our results show that the GluA1 and GluA2 subunits are modified by K63-linked polyubiquitin chains, which predominantly direct protein substrates to the lysosomes through endosomal trafficking (Nathan et al., 2013). In support of this idea, we found that GluA1 and GluA2 ubiquitin-defective mutants are inefficiently sorted into late endosomes 30 min post-internalization. This is not due to a general impairment in intracellular trafficking, as these mutants are appropriately sorted into early and recycling endosomes at 5 and 10 min post-endocytosis. In the case of GluA1, these receptors recycle back to the plasma membrane 30 min after stimulus-dependent endocytosis. As a consequence, one of our critical findings is that these ubiquitin-defective mutants are spared from agonist-induced degradation of surface AMPARs. Altogether, these results provide a demonstration of the role of direct ubiquitination of GluA1 and GluA2 subunits as a sorting signal that targets AMPARs to late endosomes for degradation.

In summary, we propose the following model for ligand-induced AMPAR trafficking (Figure 6E). First, direct binding of ligand to AMPARs causes neuronal depolarization and the opening of L-VGCCs that allows Ca^{2+} influx into the post-synaptic compartment. The rise in intracellular Ca^{2+} activates CaMKII that potentially leads to the activation and/or recruitment of E3-ligase(s) through a protein phosphorylation mechanism. Surface AMPARs are internalized without ubiquitination but are subsequently ubiquitinated, either by an E3 ligase that co-exists on the GluA1/2-containing vesicles or one that resides in the early endosomes. Ubiquitinated AMPARs are then sorted to late endosomes and degraded in the lysosomes. Our study therefore provides systematic and mechanistic insights into the role of ubiquitination in regulating activity-dependent AMPAR sorting and trafficking to ensure a homeostatic balance of receptor content in neurons, which may be crucial for synaptic plasticity, learning, and memory (Cajigas et al., 2010).

EXPERIMENTAL PROCEDURES

DNA Constructs, Antibodies, and Drugs

cDNAs encoding full-length pH-sensitive GFP, pHluorin-tagged GluA1 (pH-GluA1), and pH-GluA2 were subcloned into a vector downstream of chicken β-actin (CAG) promoter. C-terminal lysine to arginine mutants for both pH-GluA1 and pH-GluA2 were generated using the standard overlap extension PCR protocol.

Specific antibodies against GluA1 (4.9D), GluA2 (6A), GluA3 (JH4300), GluA4 (JH4303), and GFP (JH4030) were generated in the R.L.H. laboratory. The following antibodies were purchased from commercial sources: anti-ubiquitin clone P4D1 (Santa Cruz Biotechnology), anti-ubiquitin clone FK2 and anti-LAMP1 clone Ly1C6 (Enzo Lifesciences), anti-K48-linked polyubiquitin clone D9D5 and anti-K63-linked polyubiquitin clone D7A11 (Cell Signaling Technology), anti-EEA1 clone 14 (BD Transduction Laboratories), anti-syntaxin-13 clone 151.2 (Synaptic Systems), anti-a-tubulin clone B-5-1-2 (Sigma), anti-β-actin clone C4 (Millipore), and anti-PSD-95 clone K28/43 (NeuroMab). All drugs and chemicals were obtained from Tocris Biosciences or Ascent Scientific.

Neuronal Culture and Transfection

Hippocampal or cortical neurons from E18 rat pups were plated onto poly-L-lysine-coated dishes or coverslips in Neurobasal growth medium supplemented with 2% B27, 2 mM Glutamax, 50 U/ml penicillin, 50 μg/ml streptomycin, and 5% fetal bovine serum (FBS). Neurons were switched to 1% FBS (cortical) or serum-free (hippocampal) Neurobasal medium 24 hr post-seeding and fed twice a week. Cortical neurons were electroporated at DIV 0 prior to plating using the Amaxa Nucleofector II system and were used at DIV 13. Transient transfection of hippocampal neurons was performed at DIV13 using Lipofectamine 2000 (Invitrogen), and the cells were used 48 hr later. All animal procedures were approved by the University of Queensland Animal Ethics Committee.

Ubiquitination Assay

Ubiquitination of AMPARs was induced by incubating neurons in ACSF containing 40 μM bicuculline or 100 μM AMPA plus 100 μM D,L-APV and 1 μM TTX at 37°C. For the AMPA treatment, neurons were incubated with the agonist for 2 min before being returned to ACSF containing 100 μM D,L-APV and 1 μM TTX for another 8 min. In some experiments, neurons were pre-incubated with pharmacological agents in ACSF for 10–20 min at 37°C and were present throughout AMPA or bicuculline stimulation. Neurons were then lysed in warm 1% SDS (in PBS) and diluted in ten volumes of ice-cold cell lysis buffer (1% Triton X-100, 1 mM EDTA, 1 mM EGTA, 50 mM NaF, and 5 mM Na-pyrophosphate in PBS) supplemented with 10 mM NEM and Complete-EDTA free protease inhibitor cocktails (Roche). Lysates were centrifuged at 14,000 rpm for 20 min at 4°C and cleared with protein A- or G-Sepharose beads. Precleared lysates were then incubated with antibodies (anti-ubiquitin, anti-GluA1, or anti-GFP) coupled to protein A- or G-Sepharose overnight at 4°C, followed by four washes with ice-cold lysis buffer and elution in 2× SDS sample buffer. The immunoprecipitated proteins were resolved by SDS-PAGE and probed by

western blot analysis with specific antibodies against GluA1, GluA2, GluA3, GluA4, and ubiquitin.

To determine whether ubiquitination occurs on the surface fraction, neurons were first incubated with 1 mg/ml Sulfo-NHS-SS-Biotin (Pierce) for 30 min on ice, followed by two washes with ice-cold Tris-buffered saline to quench excess free biotin. Neurons were then returned to growth medium and treated with bicuculline or AMPA for 10 min. Subsequently, cells were lysed and sonicated in RIPA buffer and twice incubated with Neutravidin beads (Pierce) for 3 hr at 4°C to completely remove labeled surface proteins. Unbound lysates (flow through) were then immunoprecipitated with anti-ubiquitin antibodies and eluted in 2× SDS sample buffer. Bound proteins were analyzed by western blot with specific antibodies against GluA1–4.

Surface Staining and Antibody-Feeding Assays

Cultured hippocampal neurons were transfected with pH-GluA1 or pH-GluA2 constructs, either WT or ubiquitin-deficient mutants. Surface pH-tagged receptors were labeled with rabbit anti-GFP for 30 min at 4°C prior to fixation. The surface and total receptors were visualized by Alexa-Fluor-568-conjugated anti-rabbit secondary antibody and the endogenous GFP signal, respectively. To determine the amount of receptor internalization, surface pH-GluA1/2 was first labeled with rabbit anti-GFP antibody in live neurons for 15 min at 37°C. Neurons were then incubated in medium containing 100 μM AMPA plus 100 μM D,L-APV and 1 μM TTX for 2 min before being returned to growth medium containing 100 μM D,L-APV and 1 μM TTX for another 8 min to allow for receptor internalization. The remaining surface GFP antibody was stained with Alexa Fluor 568 secondary antibody under non-permeabilizing conditions (surface), and internalized GFP antibody was labeled with Alexa Fluor 647 secondary antibody once neurons were permeabilized (internalized). Total pH-GluA1/2 expression was visualized by endogenous GFP signal (total).

For co-localization of internalized AMPARs with endosomal protein markers, transfected hippocampal neurons were incubated with anti-GFP antibody to label surface receptors. Neurons were then treated with agonist as above, incubated for various times at 37°C in growth medium, and fixed with 4% paraformaldehyde/4% sucrose in PBS. The remaining surface GFP antibody was blocked with Alexa 488 secondary antibody, permeabilized, blocked, and incubated with primary mouse monoclonal antibodies against EEA1, syntaxin-13, and LAMP-1. The internalized receptors and endosome markers were visualized by Alexa-Fluor-568-conjugated anti-rabbit and Alexa-Fluor-647-conjugated anti-mouse secondary antibodies, respectively. For the late endosome experiments, leupeptin (100 μg/ml) was included to block lysosomal degradation of the receptors.

Quantitative immunofluorescence was performed by collecting images with a 63× oil-immersion objective on a Zeiss LSM510 confocal microscope and analyzed using Image J software (NIH). Data were expressed as the surface/total ratio or as an internalization index (internalized/(surface + internalized)). Quantification of overlapping signals was performed using a co-localization algorithm (Imaris; Bitplane) on thresholded 3D images and calculating the number of double-positive voxels/total number of internalized receptor voxels. Thresholding was kept constant for each condition.

Immunocytochemistry

For co-localization of internalized AMPARs with endosomal protein markers, transfected hippocampal neurons were incubated with anti-GFP antibody to label surface receptors. Neurons were incubated in medium containing 100 μM AMPA plus 100 μM D,L-APV and 1 μM TTX for 2 min before being returned to growth medium containing 100 μM D,L-APV and 1 μM TTX for another 3, 7, or 28 min to allow for receptor internalization, after which they were fixed with 4% paraformaldehyde/4% sucrose in PBS. The remaining surface GFP antibody was blocked with Alexa 488 secondary antibody, permeabilized, blocked, and incubated with primary mouse monoclonal antibodies against EEA1, syntaxin-13, and LAMP-1. The internalized receptors and endosomal markers were visualized by Alexa-Fluor-568-conjugated anti-rabbit and Alexa-Fluor-647-conjugated anti-mouse secondary antibodies, respectively. For the late endosome experiments, leupeptin (100 μg/ml) was included to block lysosomal degradation of the receptors. Quantitative immunofluorescence imaging was performed by collecting images with a 63× oil-immersion objective on a Zeiss LSM510 confocal microscope and analyzed using Image J software (NIH) as previously described (Anggono et al., 2013).

Receptor Degradation Assay

To measure the agonist-induced degradation of pH-GluA1 and pH-GluA2, electroporated neurons were biotinylated as described previously (Anggono et al., 2011). Neurons were treated with AMPA for 10 min, lysed, and incubated with neutravidin beads. Total cell lysates and bound proteins were analyzed by western blot with specific antibodies against GFP and α-tubulin or β-actin. The relative abundance of pH-tagged receptors was calculated as the fraction of biotinylated receptors remained (AMPA-treated/total labeled receptors) after normalizing against the total expression levels.

Protein Turnover Assay

To measure the basal protein turnover of pH-GluA1 and pH-GluA2, electroporated neurons were incubated in growth medium containing DMSO or 50 μg/ml cycloheximide at DIV13 for 24 hr, prior to lysis in 1× SDS sample buffer. Neuronal lysates were resolved by SDS-PAGE and analyzed by western blot with specific antibodies against GFP and α-tubulin. The relative abundance of pH-tagged receptors was calculated as the fraction of total receptors (cycloheximide/DMSO) after normalizing against α-tubulin levels.

Electrophysiology

Transfected hippocampal pyramidal neurons were targeted for whole-cell patch-clamp recording with borosilicate electrodes (3–6 MΩ) at room temperature in normal ACSF containing 100 μM picrotoxin, 100 μM D,L-APV, and 1 μM TTX as described previously (Anggono et al., 2011). The electrode internal solution contained (in mM): 130 cesium methanesulfonate, 10 HEPES, 0.5 EGTA, 8 CsCl,5 TEA-Cl, 1 QX-314, 10 Naphosphocreatine, 0.5 Na-GTP, and 4 Mg-ATP. Data were acquired with a Multiclamp 700A amplifier (Molecular Devices) at 4 KHz and analyzed using Axograph software (Axon Instruments). Events having amplitudes of >2.5 rms noise were averaged, and kinetic measurements were performed using a monoexponential decay function.

Supplementary Material

Refer to Web version on PubMed Central for supplementary material.

Acknowledgments

This work was supported by grants from the John T. Reid Charitable Trusts (to V.A.) and the NIH (to R.L.H.). V.A. was supported by fellowships from the International Human Frontier Science Program (LT00399/2008-L) and the Australian National Health and Medical Research Council (ID 477108). We thank Rowan Tweedale for manuscript editing and Luke Hammond and Daniel Matthews for assistance with microscopy and image analysis. Under a licensing agreement between Millipore Corporation and The Johns Hopkins University, R.L.H. is entitled to a share of royalties received by the university on sales of products described in this article. R.L.H. is a paid consultant to Millipore Corporation.

References

Anggono V, Huganir RL. 2012; Regulation of AMPA receptor trafficking and synaptic plasticity. Curr Opin Neurobiol. 22:461–469. [PubMed: 22217700]

Anggono V, Clem RL, Huganir RL. 2011; PICK1 loss of function occludes homeostatic synaptic scaling. J Neurosci. 31:2188–2196. [PubMed: 21307255]

Anggono V, Koç-Schmitz Y, Widagdo J, Kormann J, Quan A, Chen CM, Robinson PJ, Choi SY, Linden DJ, Plomann M, Huganir RL. 2013; PICK1 interacts with PACSIN to regulate AMPA receptor internalization and cerebellar long-term depression. Proc Natl Acad Sci USA. 110:13976–13981. [PubMed: 23918399]

Burbea M, Dreier L, Dittman JS, Grunwald ME, Kaplan JM. 2002; Ubiquitin and AP180 regulate the abundance of GLR-1 glutamate receptors at postsynaptic elements in C. elegans. Neuron. 35:107–120. [PubMed: 12123612]

Cajigas IJ, Will T, Schuman EM. 2010; Protein homeostasis and synaptic plasticity. EMBO J. 29:2746–2752. [PubMed: 20717144]

Carroll RC, Beattie EC, Xia H, Lüscher C, Altschuler Y, Nicoll RA, Malenka RC, von Zastrow M. 1999; Dynamin-dependent endocytosis of ionotropic glutamate receptors. Proc Natl Acad Sci USA. 96:14112–14117. [PubMed: 10570207]

Ehlers MD. 2000; Reinsertion or degradation of AMPA receptors determined by activity-dependent endocytic sorting. Neuron. 28:511–525. [PubMed: 11144360]

Ehlers MD. 2003; Activity level controls postsynaptic composition and signaling via the ubiquitin-proteasome system. Nat Neurosci. 6:231–242. [PubMed: 12577062]

Fu AK, Hung KW, Fu WY, Shen C, Chen Y, Xia J, Lai KO, Ip NY. 2011; APC(Cdh1) mediates EphA4-dependent downregulation of AMPA receptors in homeostatic plasticity. Nat Neurosci. 14:181–189. [PubMed: 21186356]

Govers R, ten Broeke T, van Kerkhof P, Schwartz AL, Strous GJ. 1999; Identification of a novel ubiquitin conjugation motif, required for ligand-induced internalization of the growth hormone receptor. EMBO J. 18:28–36. [PubMed: 9878047]

Haglund K, Dikic I. 2005; Ubiquitylation and cell signaling. EMBO J. 24:3353–3359. [PubMed: 16148945]

Haugsten EM, Malecki J, Bjørklund SM, Olsnes S, Wesche J. 2008; Ubiquitination of fibroblast growth factor receptor 1 is required for its intracellular sorting but not for its endocytosis. Mol Biol Cell. 19:3390–3403. [PubMed: 18480409]

Hell JW. 2014; CaMKII: claiming center stage in postsynaptic function and organization. Neuron. 81:249–265. [PubMed: 24462093]

Hershko A, Ciechanover A. 1998; The ubiquitin system. Annu Rev Biochem. 67:425–479. [PubMed: 9759494]

Hou Q, Gilbert J, Man HY. 2011; Homeostatic regulation of AMPA receptor trafficking and degradation by light-controlled single-synaptic activation. Neuron. 72:806–818. [PubMed: 22153376]

Huang F, Goh LK, Sorkin A. 2007; EGF receptor ubiquitination is not necessary for its internalization. Proc Natl Acad Sci USA. 104:16904–16909. [PubMed: 17940017]

Huganir RL, Nicoll RA. 2013; AMPARs and synaptic plasticity: the last 25 years. Neuron. 80:704–717. [PubMed: 24183021]

Lee SH, Simonetta A, Sheng M. 2004; Subunit rules governing the sorting of internalized AMPA receptors in hippocampal neurons. Neuron. 43:221–236. [PubMed: 15260958]

Lin A, Hou Q, Jarzylo L, Amato S, Gilbert J, Shang F, Man HY. 2011; Nedd4-mediated AMPA receptor ubiquitination regulates receptor turnover and trafficking. J Neurochem. 119:27–39. [PubMed: 21338354]

Lu W, Roche KW. 2012; Posttranslational regulation of AMPA receptor trafficking and function. Curr Opin Neurobiol. 22:470–479. [PubMed: 22000952]

Lussier MP, Nasu-Nishimura Y, Roche KW. 2011; Activity-dependent ubiquitination of the AMPA receptor subunit GluA2. J Neurosci. 31:3077–3081. [PubMed: 21414928]

Lussier MP, Herring BE, Nasu-Nishimura Y, Neutzner A, Karbowski M, Youle RJ, Nicoll RA, Roche KW. 2012; Ubiquitin ligase RNF167 regulates AMPA receptor-mediated synaptic transmission. Proc Natl Acad Sci USA. 109:19426–19431. [PubMed: 23129617]

Mabb AM, Ehlers MD. 2010; Ubiquitination in postsynaptic function and plasticity. Annu Rev Cell Dev Biol. 26:179–210. [PubMed: 20604708]

Macia E, Ehrlich M, Massol R, Boucrot E, Brunner C, Kirchhausen T. 2006; Dynasore, a cell-permeable inhibitor of dynamin. Dev Cell. 10:839–850. [PubMed: 16740485]

Nathan JA, Kim HT, Ting L, Gygi SP, Goldberg AL. 2013; Why do cellular proteins linked to K63-polyubiquitin chains not associate with proteasomes? EMBO J. 32:552–565. [PubMed: 23314748]

Patrick GN, Bingol B, Weld HA, Schuman EM. 2003; Ubiquitin-mediated proteasome activity is required for agonist-induced endocytosis of GluRs. Curr Biol. 13:2073–2081. [PubMed: 14653997]

Schwarz LA, Hall BJ, Patrick GN. 2010; Activity-dependent ubiquitination of GluA1 mediates a distinct AMPA receptor endocytosis and sorting pathway. J Neurosci. 30:16718–16729. [PubMed: 21148011]

Shepherd JD, Huganir RL. 2007; The cell biology of synaptic plasticity: AMPA receptor trafficking. Annu Rev Cell Dev Biol. 23:613–643. [PubMed: 17506699]

Sorkin A, von Zastrow M. 2009; Endocytosis and signalling: intertwining molecular networks. Nat Rev Mol Cell Biol. 10:609–622. [PubMed: 19696798]

Yuen EY, Wei J, Liu W, Zhong P, Li X, Yan Z. 2012; Repeated stress causes cognitive impairment by suppressing glutamate receptor expression and function in prefrontal cortex. Neuron. 73:962–977. [PubMed: 22405206]

Zhang D, Hou Q, Wang M, Lin A, Jarzylo L, Navis A, Raissi A, Liu F, Man HY. 2009; Na,K-ATPase activity regulates AMPA receptor turnover through proteasome-mediated proteolysis. J Neurosci. 29:4498–4511. [PubMed: 19357275]

Highlights

- All AMPA receptor subunits (GluA1-4) are ubiquitinated upon neuronal activity
- Ubiquitination of AMPA receptors requires the activity of LVGCCs and CaMKII
- GluA1 and GluA2 are ubiquitinated on K868 and K870/K882 in the C terminus
- Ubiquitination regulates post-endocytic sorting and degradation of AMPA receptors

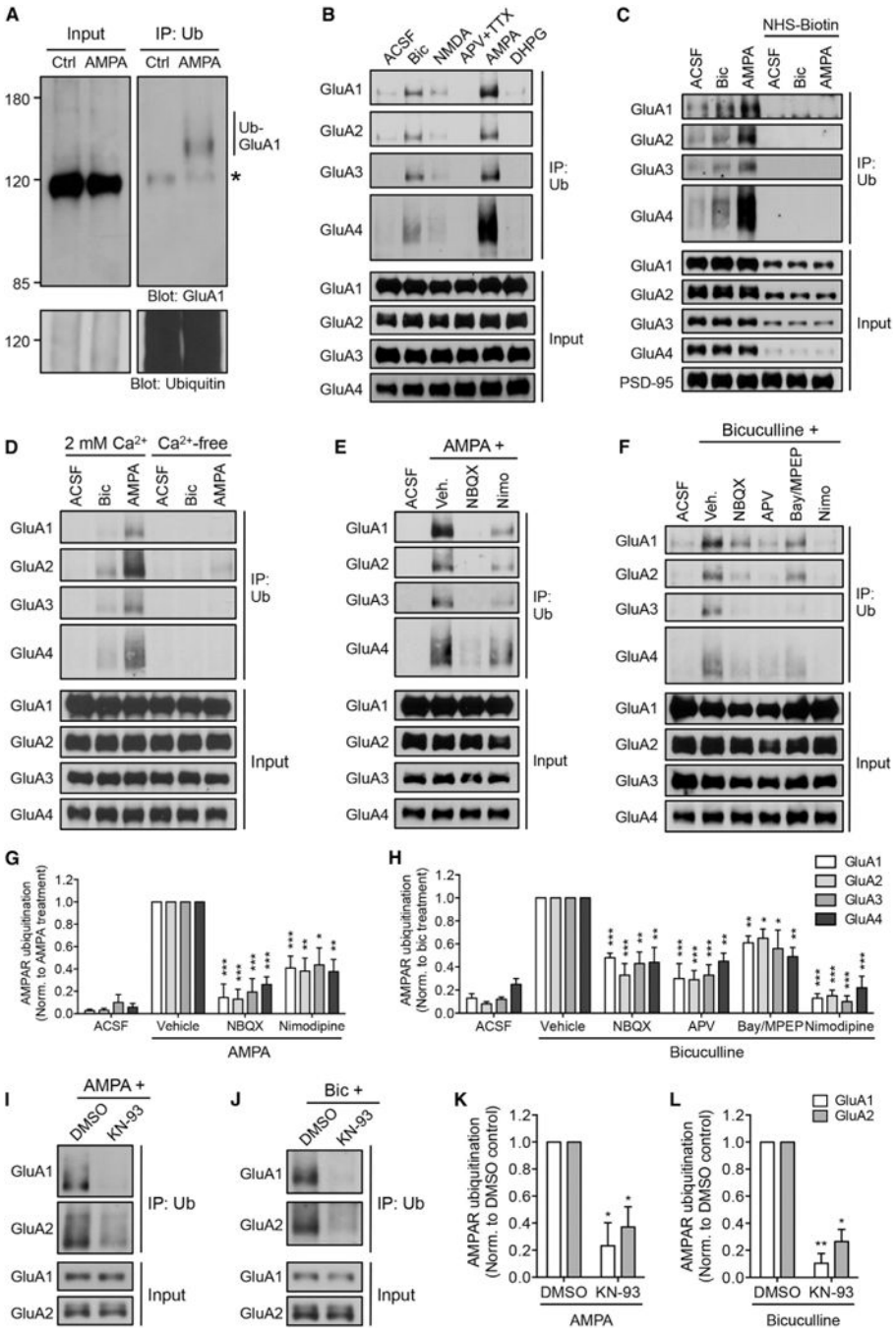

Figure 1. Activity-Dependent Ubiquitination of All AMPAR Subunits Requires Neuronal Depolarization and Ca^{2+}

(A) Cortical neurons were incubated in ACSF in the presence or absence of 100 μM AMPA plus 100 μM D,L-APV and 1 μM TTX for 2 min. The AMPA-treated neurons were immediately incubated in ACSF containing 100 μM D,L-APV and 1 μM TTX for a further 8 min at 37°C. This protocol is referred to as 100 μM AMPA treatment hereafter. Neurons were then lysed in 1% SDS and immunoprecipitated using anti-ubiquitin antibodies (IP: Ub). Eluted proteins were subjected to western blot analysis and probed with anti-ubiquitin and anti-GluA1 antibodies. * denotes non-specific band.

(B) Cortical neurons were incubated in ACSF in the absence or presence of glutamate receptor agonists (20 μM NMDA+ 1 μMTTX, 100 μM AMPA + 100 μM D,L-APV and 1 μM TTX, or 100 μM DHPG + 1 μM TTX), 40 μM bicuculline (bic), or 100 μM D,L-APV and 1 μM TTX for 10 min at 37°C. They were then lysed and immunoprecipitated with anti-ubiquitin antibodies and probed with specific antibodies against the GluA1-GluA4 subunits of AMPARs.

(C) Surface receptors in cortical neurons were biotinylated at 4°C prior to bicuculline or AMPA stimulation for 10 min at 37°C. Cell lysates were pre-incubated with neutravidin beads prior to immunoprecipitation with anti-ubiquitin antibodies.

(D) Cortical neurons were incubated in ACSF containing 2 mM Ca^{2+} or 0 mM Ca^{2+} + 50 μM BAPTA-AM + 2 mM EGTA (Ca^{2+}-free) for 20 min before the addition of bicuculline or AMPA for 10 min at 37°C. Cells were lysed and immunoprecipitated with anti-ubiquitin antibodies.

(E–H) Cortical neurons were incubated with the indicated inhibitors (vehicle [Veh.], 10 μM NBQX, 10 μM nimodipine[Nimo], 100 μM D,L-APV, and 10 μM Bay 36-7620 + 5 μM MPEP [Bay/MPEP]) for 10 min before adding AMPA(E) or bicuculline (F) for another 10 min at 37°C. (G and H) The effects of these inhibitors on AMPAR ubiquitination were quantified and normalized to vehicle controls (ANOVA; *$p < 0.05$; **$p < 0.01$; ***$p < 0.001$; $n = 3–6$ per group). Data represent mean ± SEM.

(I–L) Cortical neurons were incubated with either DMSO or the CaMKII inhibitor, KN-93(10 μM), for 10 min before adding AMPA (I) or bicuculline (J) for 10 min at 37°C. (K and L) The effects of KN-93 on AMPAR ubiquitination were quantified and normalized to DMSO controls (t test; *$p < 0.05$; **$p < 0.01$; $n = 3$ to 4 per group). Data represent mean ± SEM.

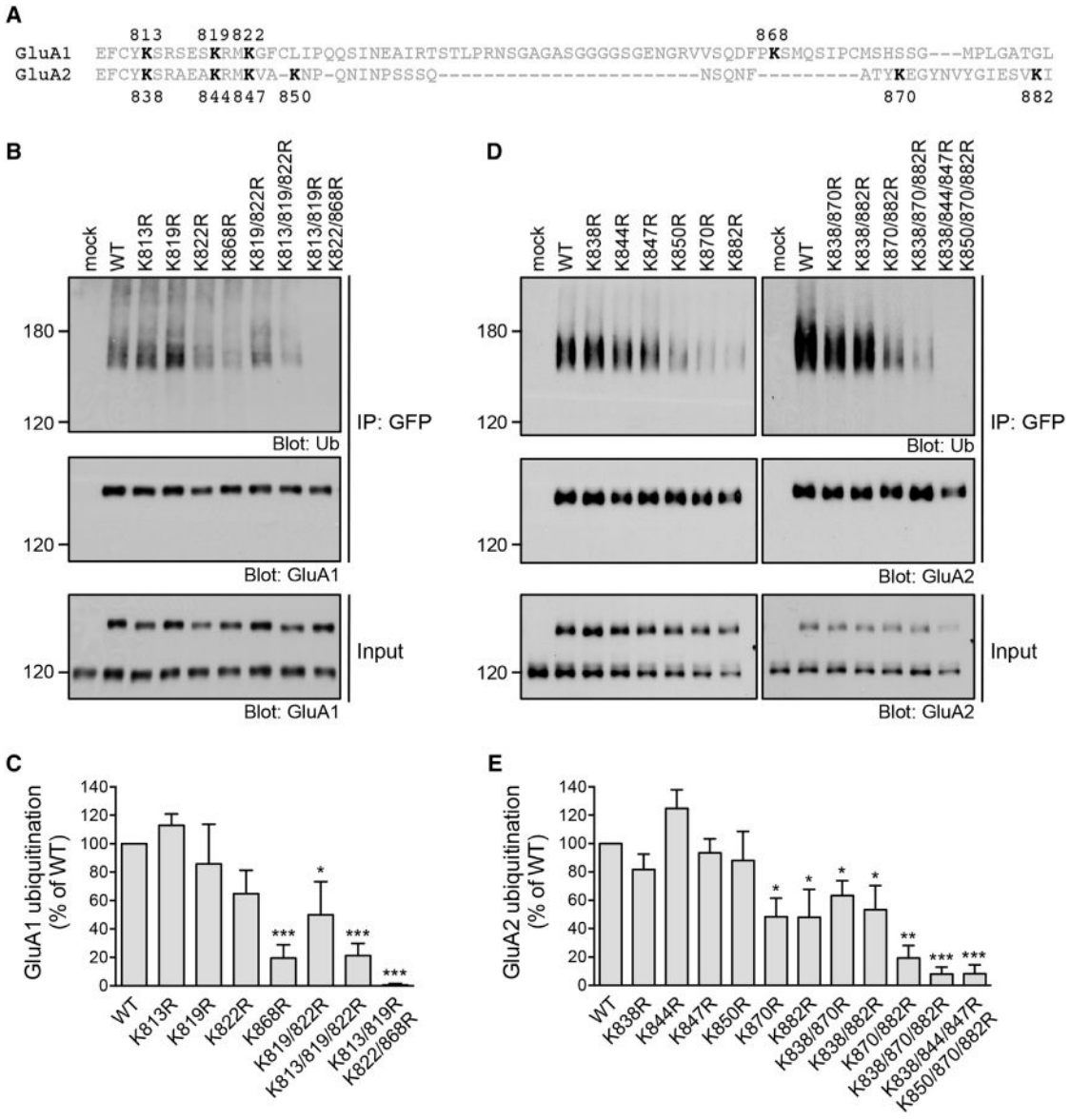

Figure 2. The GluA1 and GluA2 Subunits of AMPARs Are Ubiquitinated on Lysine Residues in Their Carboxy Tails

(A) The amino acid sequence alignment of the GluA1 and GluA2 C termini, with all lysine residues highlighted in black.

(B–E) Cortical neurons were electroporated with pH-GluA1 (B) or pH-GluA2 (D) constructs, either wild-type (WT) or mutants in which the lysine residues have been substituted to arginines individually or in combination, prior to plating. At DIV13, the neurons were treated with AMPA for 10min at 37°C, lysed in 1% SDS, and immunoprecipitated using anti-GFP antibodies. Eluted proteins were subjected to western blot analysis and probed with anti-ubiquitin and anti-GluA1 antibodies. The effects of these Lys/Arg mutants on pH-GluA1 (C) and pH-GluA2 (E) ubiquitination were quantified after normalizing against the amount of immunoprecipitated receptor. Data represent mean ±

SEM of band intensities normalized to control values of WT neurons (ANOVA; *$p < 0.05$; **$p < 0.01$; ***$p < 0.001$; $n = 3$ to 4 per group).

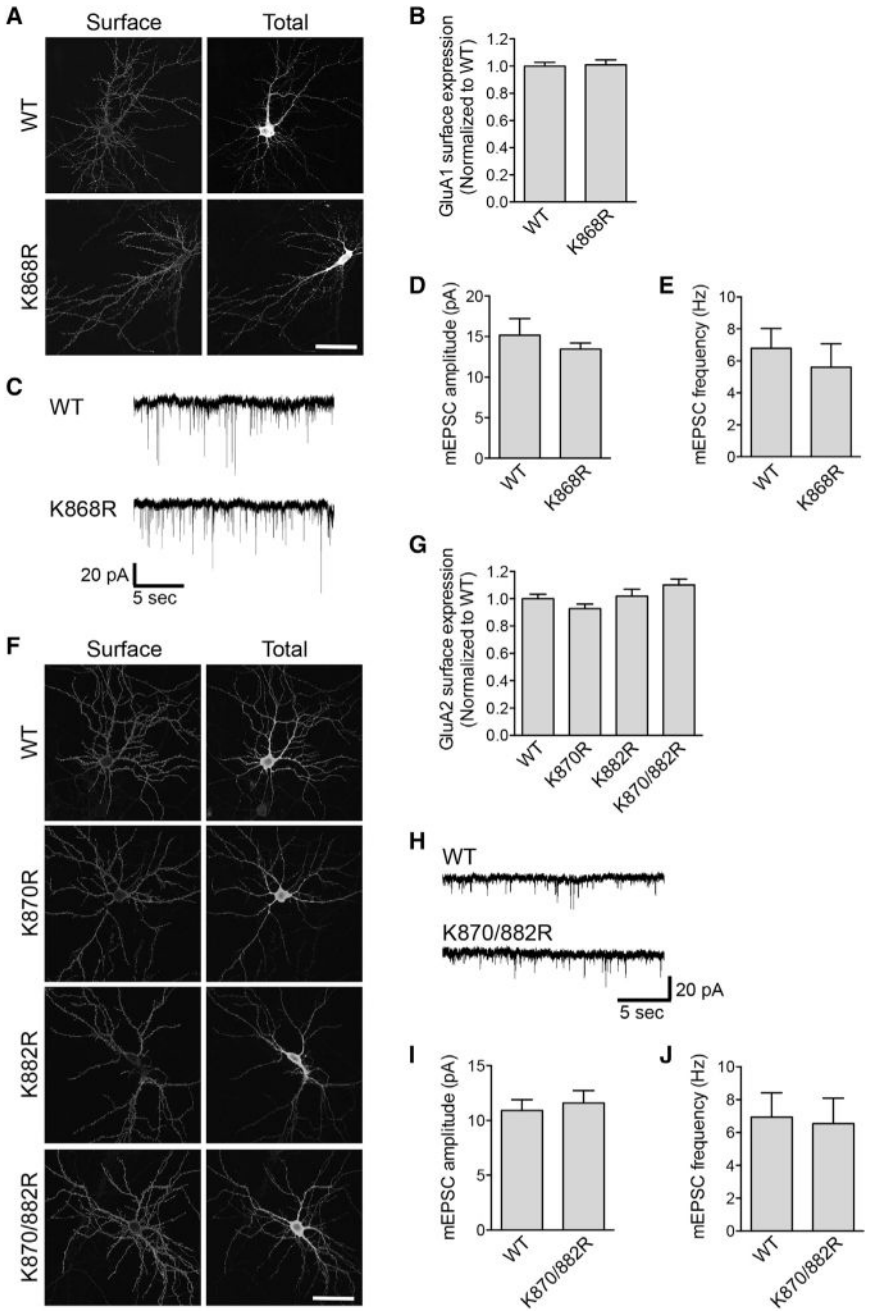

Figure 3. Ubiquitination of GluA1 and GluA2 Does Not Regulate Steady-State Expression of AMPARs

Cultured hippocampal neurons were transfected with pH-GluA1, either WT or the ubiquitin-deficient K868R mutant, at DIV13. At DIV15, surface pH-GluA1 was labeled with rabbit-anti GFP antibody for 30 min at 4°C before fixation. Surface pH-GluA1 was visualized by immunostaining with Alexa Fluor 568 anti-rabbit antibodies, whereas total pH-GluA1 was visualized by the endogenous GFP signal.

(A) Representative images of surface and total pH-GluA1 in a neuron from each group. The scale bar represents 50 μm.

(B) Quantification of the surface/total pH-GluA1 ratio normalized to the value of WT neurons (n = 31 neurons per group).
(C) Representative whole-cell recording sample traces of mEPSC events from each group.
(D and E) Quantification of mean mEPSC amplitude (D) and frequency (E) for each population. Data represent mean ± SEM (n = 7 neurons per group).
(F–J) Hippocampal neurons transfected with pH-GluA2 ubiquitin-deficient mutants did not display any significant difference in the surface/total receptor ratios (F and G; n = 17–44 neurons per group) or mEPSC amplitude and frequency (H–J; n = 9 to 10 neurons per group). The scale bar represents 50 μm.

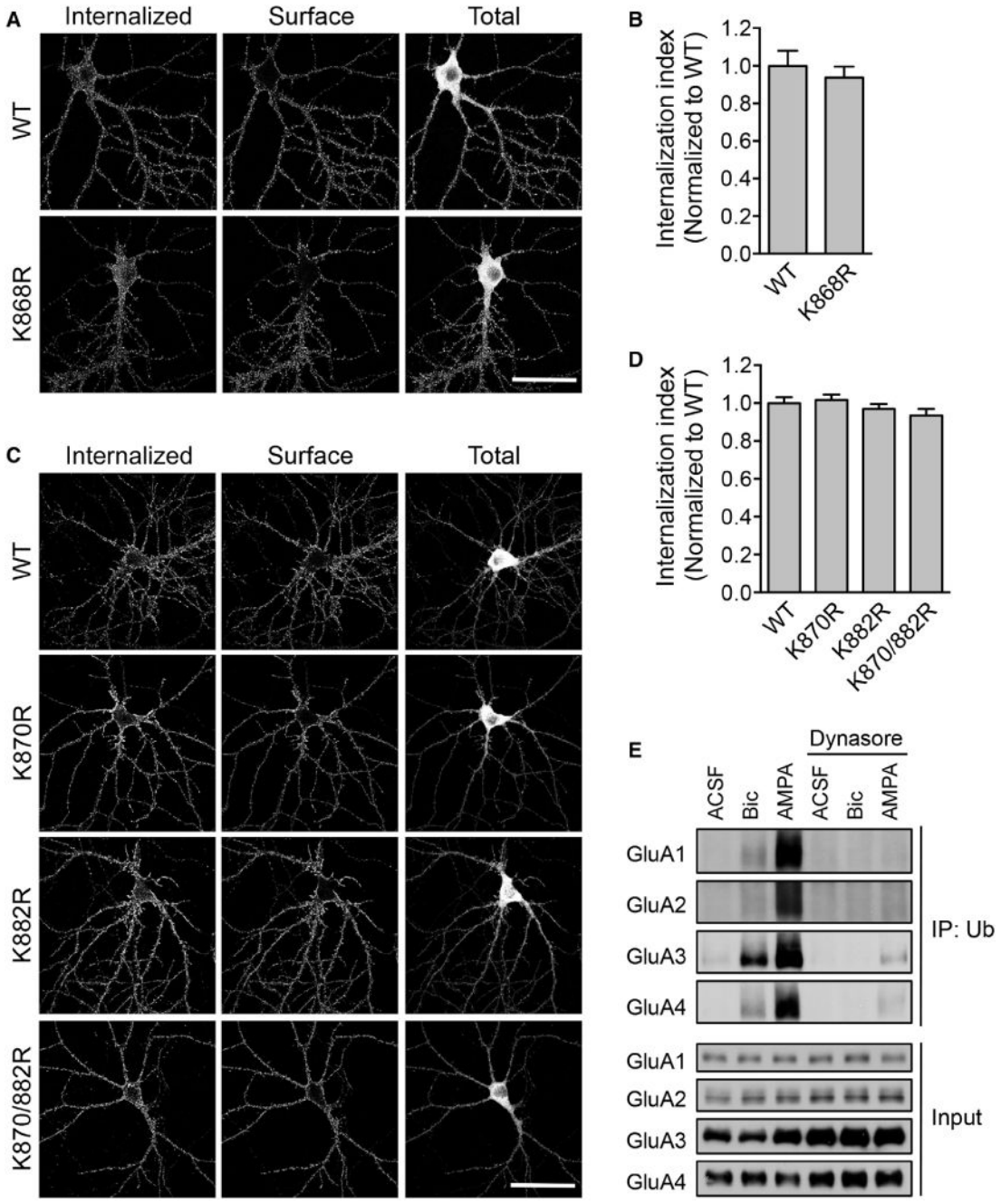

Figure 4. Ubiquitination of GluA1 and GluA2 Is Not Required for the Ligand-Induced Endocytosis of AMPARs

(A) Cultured hippocampal neurons were transfected with pH-GluA1, either WT or ubiquitin-deficient K868R mutant, at DIV13. At DIV15, surface pH-GluA1 was labeled with rabbit anti-GFP antibody for 15 min at 37°C followed by a 10 min incubation with 100 μM AMPA to induce receptor internalization. The remaining surface GFP antibody was stained with Alexa Fluor 568 secondary antibody under non-permeabilizing conditions (surface), and internalized GFP antibody was labeled with Alexa Fluor 647 secondary

antibody (internalized). Total pH-GluA1 expression was visualized by the endogenous GFP signal. The scale bar represents 50 μm.

(B) The internalization of pH-GluA1 was measured as the ratio of internalized/(internalized + surface) fluorescence (internalization index), normalized to the WT control. Data represent mean ± SEM (n = 11–13 neurons per group).

(C and D) Hippocampal neurons transfected with pH-GluA2 ubiquitin-deficient mutants exhibited normal endocytosis following the application of AMPA(C), as shown by the internalization index (D) for each group. Data represent mean ± SEM (n = 27–34 neurons per group). The scale bar in (C) represents 50 μm.

(E) Cortical neurons were incubated with an endocytosis inhibitor, dynasore(80 μM), for 10 min before the addition of bicuculline or AMPA for another 10 min at 37°C. Neurons were lysed and immunoprecipitated with anti-ubiquitin antibodies. Eluted proteins were subjected to western blot analysis and probed with specific antibodies against all four AMPAR subunits, GluA1–4.

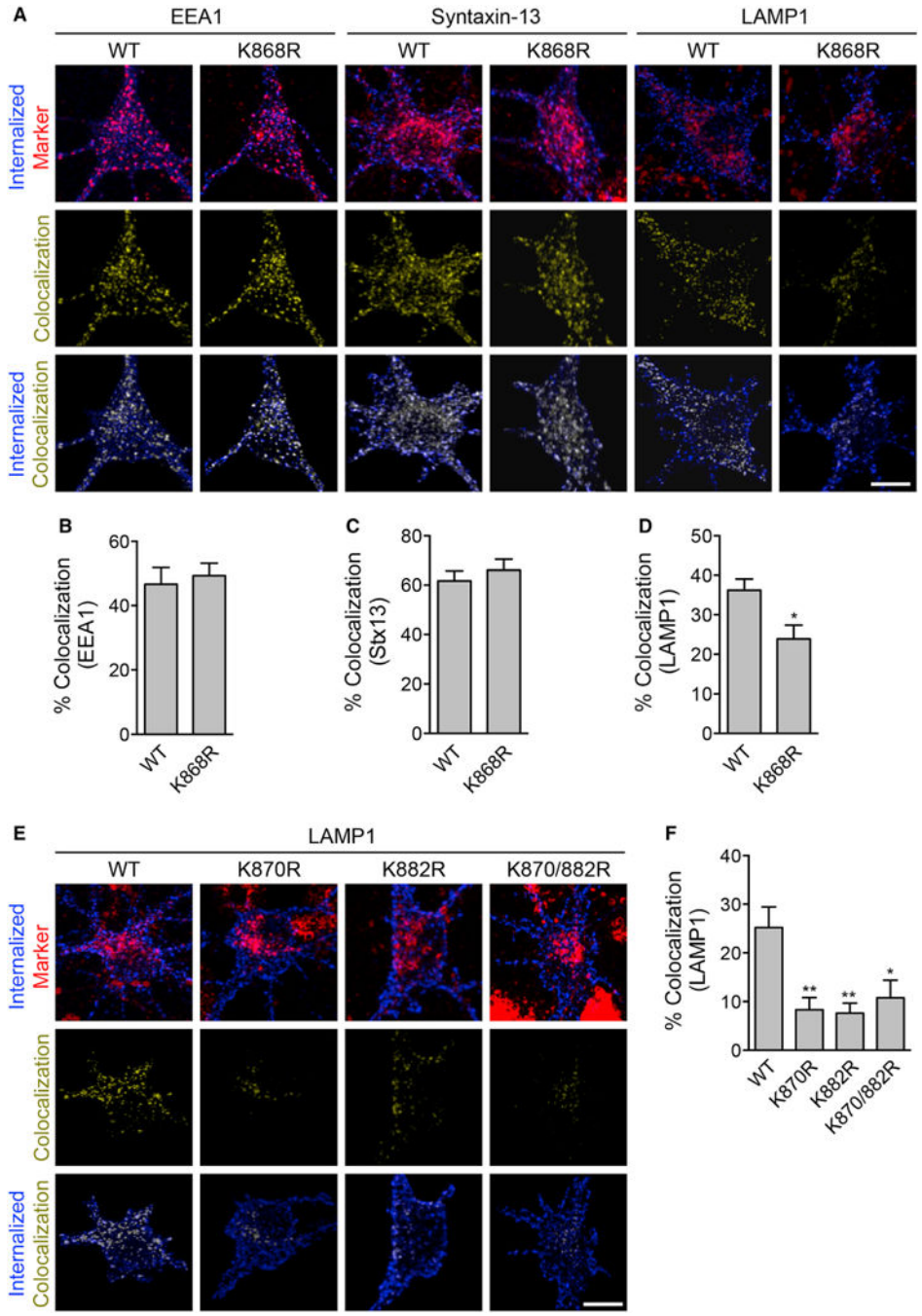

Figure 5. Ubiquitination of GluA1 and GluA2 Regulates the Ligand-Induced Intracellular Sorting of Internalized AMPARs to Late Endosomes

(A) Hippocampal neurons were transiently transfected with pH-GluA1, either WT or the ubiquitin-deficient mutant K868R, at DIV13 for 48 hr. The neurons were then labeled with anti-GFP antibodies, stimulated with AMPA for 2 min, and returned to growth medium for 3 min (early endosomes), 8 min (recycling endosomes), or 28 min (late endosomes) to allow for GluA1 internalization (blue) and sorting into different endosomal compartments (magenta). Simultaneous staining for the early endosome marker, EEA1 (left panels), the recycling endosome marker, syntaxin-13 (middle panels), and the late endosome marker,

LAMP1 (right panels), revealed co-localization (yellow) with internalized pH-GluA1 after AMPA application. The scale bar represents 10 μm.

(B–D) The extent of association of internalized pH-GluA1 with EEA1- (B), Stx13- (C), and LAMP1-labeled compartments (D) was quantified by image analysis as a percentage of co-localized signals over the amount of total internalized receptors. Data represent mean ± SEM (t test; *$p < 0.05$; n = 6–14 neurons per group). (E and F) Representative images (E) and quantification (F) of LAMP1-positive endosome co-localization with internalized pH-GluA2, either WT or ubiquitin-deficient mutants (K870R, K882R, and K870/882R), 30 min after AMPA treatment. The scale bar represents 10 μm. Data represent mean ± SEM (ANOVA; *$p < 0.05$; **$p < 0.01$; n = 13–16 neurons per group).

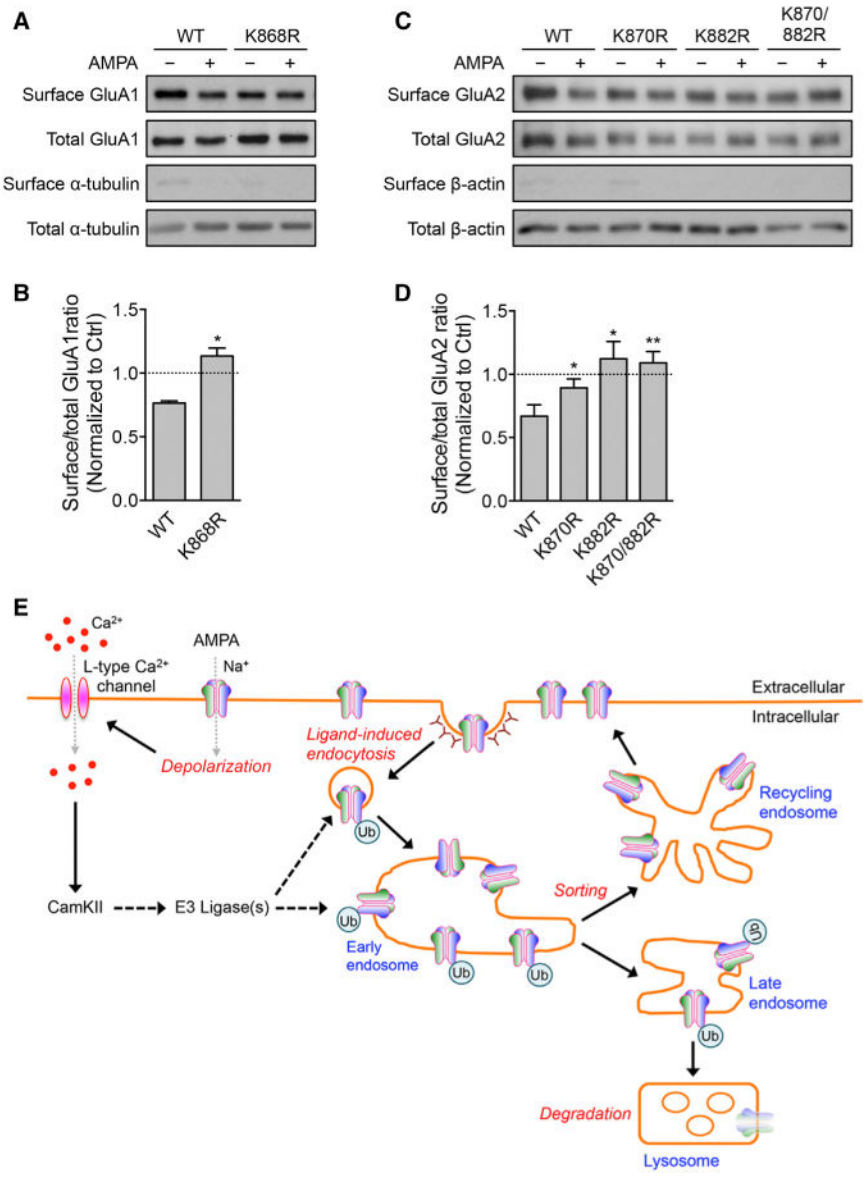

Figure 6. Ubiquitination of GluA1 and GluA2 Is Required for Ligand-Induced Degradation of AMPARs

(A–D) Cortical neurons were electroporated with pH-GluA1 (A) and pH-GluA2 (C) constructs, either WT or ubiquitin-deficient mutants as indicated, prior to plating. At DIV13, surface receptors were biotinylated and immediately lysed in RIPA buffer to determine the total amount of biotinylated surface receptors. Sister neuronal cultures were subsequently treated with AMPA for 5 min and returned to growth medium for 90 min at 37°C prior to cell lysis. Neuronal lysates were then incubated with neutravidin beads. Eluted proteins were subjected to western blot analysis and probed with anti-GFP, anti-a-tubulin, and anti-β-actin antibodies. The effects of these mutants on agonist-induced pH-GluA1 (B) and pH-GluA2 (D) degradation were quantified as surface/total receptor ratios and expressed as fractions of remaining receptors after AMPA treatment. Data represent mean ± SEM (t test or ANOVA; *$p < 0.05$; **$p < 0.01$; n = 5 to 6 per group).

(E) Proposed model for the role of protein ubiquitination in mediating AMPAR endocytic sorting. In this model, activation of AMPARs by the agonist leads to neuronal depolarization and endocytosis of AMPARs into early endosomes. Ligand-induced AMPAR ubiquitination requires Ca^{2+} influx through L-type voltage-gated Ca^{2+} channels and CaMKII activity. The latter may activate E3 li-gases such as Nedd4-1, RNF147, or APC^{Cdh1} to ubiquitinate internalized AMPARs, perhaps in the early endosomes. Ubiquitinated receptors are targeted to late endosomes and are subsequently degraded by lysosomes.